JOURNAL OF GEOPHYSICAL RESEARCH, VOL. 104, NO. A3, PAGES 4447–4455, MARCH 1, 1999

Magnetic mirroring in an incident proton beam

Marina Galand[1] and Arthur D. Richmond

High Altitude Observatory, National Center for Atmospheric Research, Boulder, Colorado

Abstract. We point out that the influence of magnetic-field nonuniformity on redirecting the pitch angle of a particle is independent of the particle's charge and thus is identical for protons and neutral hydrogen atoms. Under certain circumstances one can then speak of "magnetic mirroring" of hydrogen atoms as well as of protons. In the case of an energetic proton beam incident on the upper atmosphere, the study of the influence of magnetic field on both protons and H atoms can be relevant to inferring information about proton aurora from measurements of upgoing energetic particles observed from space. In a model that here neglects collisional angular redistribution of the particles, the total particle and energy albedos are approximately independent of the energy of the incident particles and of the atmospheric temperature. However, the separate proton and H atom albedos have a strong dependence on the incident energy. We also reinvestigate how to handle energy conservation properly in the presence of a nonuniform magnetic field, to provide a good validation for proton transport models.

1. Introduction

Energetic proton precipitation into the auroral upper atmosphere can at times be a significant source of ionization [*Basu et al.*, 1987; *Senior et al.*, 1987; *Lilensten and Galand*, 1998] and of measurable auroral hydrogen-line emissions [e.g., *Eather*, 1967; *Søraas et al.*, 1974; *Henriksen et al.*, 1985; *Sigernes et al.*, 1996; *Deehr et al.*, 1998]. Through charge-changing reactions the protons capture electrons from neutral atmosphere species (typically, N_2, O_2, and O) to become energetic neutral hydrogen atoms and later usually lose the electrons again to reemerge as energetic protons [e.g., *Basu et al.*, 1993]. This cycle can repeat many times for each energetic particle.

The pitch angle of an energetic particle, defined as the angle between its velocity vector and the magnetic field vector (or, sometimes, the direction opposite to the magnetic field), changes both from the cumulative effect of small collisional deflections [e.g., *Galand et al.*, 1998] and from the movement of the particle through the nonuniform magnetic field [e.g., *Kozelov*, 1993]. Considering the latter effect applied only to the protons but not the H atoms, *Galand et al.* [1998] found, in studying the resultant effect on H emission profiles, that the collisional angular redistribution generally dominates over the effect of magnetic-field nonuniformity in altering the pitch angles. However, the effect of magnetic-field nonuniformity is not necessarily negligible, especially for particles that do not penetrate deeply into the upper atmosphere.

The changes in pitch angle can lead to a fraction of the particles incident on the upper atmosphere being sent back into space. Recently, measurements aboard a rocket sent through a proton aurora brought out the presence of such an upward flux composed of not only protons but also energetic neutral atoms [*Søraas and Aarsnes*, 1996]. Moreover, the presence of an upward flux opens the possibility of red-shifted hydrogen emission appearing in the proton aurora observed from the ground [e.g., *Galand et al.*, 1998]. Observations of the upgoing energetic protons and hydrogen atoms from space and of the induced red-shifted hydrogen emission from the ground, together with appropriate models, can be used to infer some properties of the proton aurora. Thus it is important to model accurately the physical processes giving rise to the upgoing particles.

For protons the continual change of pitch angle in a nonuniform magnetic field can be expressed in terms of the "magnetic mirror" effect [e.g., *Kozelov*, 1993; *Galand et al.*, 1998]. For hydrogen atoms the pitch angle change occurs not from redirection of the atom velocity, but rather from the spatially changing direction of the magnetic field through which the atom is moving [*Kozelov*, 1993]. In his analysis of pitch angle changes of H atoms, *Kozelov* [1993] treated magnetic-field lines as being vertical everywhere, which approximates the conditions in the polar ionosphere. The relation he obtained bears an analogy to the treatment of electromagnetic radiation transfer in a spherical atmosphere [e.g., *Mihalas and Mihalas*, 1984, p. 335]. The same

[1]Now at Space Environment Center, National Oceanic and Atmospheric Administration, Boulder, Colorado.

Paper number 1998JA900123.
0148-0227/99/1998JA900123$09.00

approach was repeated later by *Lorentzen et al.* [1998]. However, this magnetic-field configuration corresponds to that of a magnetic monopole, which has less spreading of field lines with increasing altitude than a dipole does. *Kozelov* [1993] found that the pitch angles of energetic H atoms change in the same sense as for mirroring protons; that is, the velocity component parallel to the magnetic field continually becomes less downward or more upward for all particles. Using a dipolar magnetic field configuration to compute the rate of change of pitch angle for protons, he found that the rates of pitch angle change are similar for the protons and H atoms, but not identical.

In this paper we reexamine how magnetic-field nonuniformity affects the pitch angles of neutral hydrogen atoms, using an identical magnetic field configuration as for protons. This results in identical mathematical relations for both types of particles, as opposed to *Kozelov*'s [1993] somewhat different relations. These new relations are then used to carry out calculations of particle and energy albedos for the idealized case of no collisional angular redistribution. We also reinvestigate the manner in which energy conservation is to be evaluated in a nonuniform magnetic field.

2. "Magnetic Mirroring" of Neutral Particles

Although the magnetic mirror effect is conventionally described in terms of the motion of the guiding center of a gyrating charged particle in a nonuniform magnetic field [e.g., *Chen*, 1983], it can also be examined from the perspective of a local effect at the actual position of a particle, without reference to the guiding center. As we show below, this perspective allows us to explain the changing pitch angle of a particle solely in terms of its motion through the nonuniform magnetic field (if forces parallel to the magnetic field are ignored), irrespective of the Lorentz force on the particle. From this perspective, the mirror effect applies equally to charged and uncharged particles. The qualitative difference between charged and uncharged particles is that the former are restricted to remain in the close vicinity of one particular magnetic-field line by the Lorentz force, while the latter may travel much farther from any particular field line before being halted as they lose an electron and become subject to the Lorentz force. Although the magnitudes of transverse displacement are different for the charged and neutral states of a particle, the pitch angle variations of both states must be taken into consideration equally. Hence we speak of "magnetic mirroring" of the neutral H atoms as well as of the protons.

Let us denote the velocity of a particle by $\mathbf{v}$, the magnetic field by $\mathbf{B}$, and a unit vector along $\mathbf{B}$ by $\mathbf{b}$. The parallel component of velocity is then

$$v_\parallel = \mathbf{b} \cdot \mathbf{v}. \tag{1}$$

Its time-rate-of-change is

$$\frac{dv_\parallel}{dt} = \frac{d(\mathbf{b} \cdot \mathbf{v})}{dt} = \mathbf{b} \cdot \frac{d\mathbf{v}}{dt} + \frac{d\mathbf{b}}{dt} \cdot \mathbf{v}. \tag{2}$$

We are concerned with cases in which there is no net force along the magnetic field, applicable to both neutral and charged particles when parallel electric fields and gravity can be neglected. For such cases the first term on the right-hand side of (2) is zero, and in a time-invariant magnetic field,

$$\frac{dv_\parallel}{dt} = \mathbf{v} \cdot \frac{d\mathbf{b}}{dt} = \mathbf{v} \cdot (\mathbf{v} \cdot \nabla)\mathbf{b} = \mathbf{v}_\perp \cdot (\mathbf{v} \cdot \nabla)\mathbf{b}, \tag{3}$$

where $\mathbf{v}_\perp$ is the component of $\mathbf{v}$ perpendicular to the magnetic field. The last step of (3) results from the fact that since $\mathbf{b}$ is by definition a unit vector, all components of its gradient, and hence $(\mathbf{v} \cdot \nabla)\mathbf{b}$, must be perpendicular to itself; that is, changes in $\mathbf{b}$ can represent only rotations and not changes of magnitude.

Let us define a Cartesian coordinate system (s,x,y) that at a particular point has its s axis parallel to $\mathbf{b}$. At this point, (3) can be expanded as

$$\frac{dv_\parallel}{dt} = v_x \left(v_x \frac{\partial b_x}{\partial x} + v_y \frac{\partial b_x}{\partial y} + v_s \frac{\partial b_x}{\partial s} \right) + v_y \left(v_x \frac{\partial b_y}{\partial x} + v_y \frac{\partial b_y}{\partial y} + v_s \frac{\partial b_y}{\partial s} \right). \tag{4}$$

This expression simplifies considerably for either of the following two idealized cases: (1) The s axis is an axis of symmetry for the magnetic field, meaning that the field line through the origin is straight and the magnetic field is axially symmetric about this line, or (2) equation (4) is averaged over a set of particles, all with the same magnitudes of total velocity (v), velocity parallel to $\mathbf{b}$ ($v_\parallel$), and velocity perpendicular to $\mathbf{b}$ ($v_\perp$), but with different azimuthal directions [$\arctan(v_x/v_y)$] that are uniformly distributed in azimuth about the s axis. We shall denote the average over such a set with an overbar ($\overline{\ }$). Case 1 is often used to illustrate magnetic mirroring of charged particles, but for a dipolar magnetic field it is strictly valid only over the magnetic poles. Case 2 corresponds to an assumption commonly made in one-dimensional modeling of the transport equation for energetic particle precipitation [e.g., *Basu et al.*, 1993; *Galand et al.*, 1997], although azimuthal isotropy of the particle distribution function is not strictly accurate when there is a horizontal gradient of the precipitating particle flux. For example, there will be more H atoms directed away from the center of a precipitating proton beam than toward the center. Thus a totally general evaluation of $dv_\parallel/dt$ would require consideration of all the terms on the right-hand side of (4). However, under most circumstances the simplification obtained by assuming either of the two idealized cases 1 or 2 captures the dominant effects of the magnetic-field geometry on $dv_\parallel/dt$. We shall assume case 2. If case 1 had been assumed, the overbars could be removed from the following equations,

which would then become valid for individual particles.

Assuming case 2 above, we average (4) over the set of particles with identical v, $v_\parallel$, and $v_\perp$ but with a uniform distribution in azimuth and find that all terms in (4) disappear that involve v_x or v_y to the first power, or the product $v_x v_y$, so that

$$\overline{\frac{dv_\parallel}{dt}} = \overline{v_x^2}\frac{\partial b_x}{\partial x} + \overline{v_y^2}\frac{\partial b_y}{\partial y} = \frac{v_\perp^2}{2}\left(\frac{\partial b_x}{\partial x} + \frac{\partial b_y}{\partial y}\right), \quad (5)$$

since by assumption $\overline{v_x^2} = \overline{v_y^2} = v_\perp^2/2$. We can add the null quantity $(v_\perp^2/2)(\partial b_s/\partial s)$ to the right-hand side of (5) (null at the point under consideration, where $\mathbf{b}$ is parallel to the s axis) to get

$$\begin{aligned}\overline{\frac{dv_\parallel}{dt}} = \frac{v_\perp^2}{2}\nabla\cdot\mathbf{b} &= \frac{v_\perp^2}{2}\nabla\cdot\left(\frac{\mathbf{B}}{B}\right) = \frac{v_\perp^2}{2}\mathbf{B}\cdot\nabla\left(\frac{1}{B}\right) \\ &= -\frac{v_\perp^2}{2B}\mathbf{b}\cdot\nabla B = -\frac{v_\perp^2}{2B}\frac{\partial B}{\partial s}. \quad (6)\end{aligned}$$

Since $v_\parallel = v\mu$ and $v_\perp = v\sqrt{1-\mu^2}$, where μ is the cosine of the pitch angle, and since v is assumed to remain constant, (6) yields

$$\overline{\frac{d\mu}{dt}} = -\frac{v(1-\mu^2)}{2B}\frac{\partial B}{\partial s}. \quad (7)$$

Dividing (7) by $v_\parallel$ then gives

$$\overline{\frac{d\mu}{ds}} = -\frac{(1-\mu^2)}{2\mu B}\frac{\partial B}{\partial s}. \quad (8)$$

(Notice that if the sign definitions of both s and μ are reversed, for example, being positive upward in the northern hemisphere, then (8) remains valid.)

Equations (6)-(8) apply to any type of particle, charged or uncharged. For charged particles they correspond to apparent magnetic-field-aligned acceleration conventionally associated with the magnetic mirror force [e.g., *Lie-Svendsen and Rees*, 1996]. A subtle difference is that we have averaged over a transversely isotropic distribution of particles at a given point, while the usual derivation of the magnetic mirror effect is obtained by considering the average magnetic force on a single particle, projected to the particle's center of gyration and averaged over one gyration. Our derivation is Eulerian, while the conventional derivation is Lagrangian. From the perspective of our derivation the magnitude and sign of $dv_\parallel/dt$ can be viewed as being caused purely by the geometry of the magnetic field, and not directly by any actual force, magnetic or otherwise.

The concept of magnetic mirroring carries with it the implication that during the time the pitch angle of a particle is changing from downward toward upward, the particle remains in the vicinity of its original field line. This condition is enforced on protons by the Lorentz force. In contrast, energetic particles that are converted back and forth between charged and neutral states will wander away from their original field line in a form of random walk. Whether this will carry them so far away from their original field line that the concept of magnetic mirroring loses usefulness will depend both on the mean step size of the random walk, that is, the distance of linear travel during the neutral state of the particles, and on the number of steps. It will also depend on the context of the problem under examination. For example, the width of the proton beam that is impinging on the upper atmosphere is a relevant factor. In reality, the horizontal transport of particles out of the beam is often significant, and this so-called beam spreading is sometimes crudely treated in one-dimensional numerical modeling by use of an attenuation factor applied to the center of the beam [*Jasperse and Basu*, 1982].

Figure 1 illustrates the nature of the random walk and the upward net acceleration on the energetic particles. In order to stress the "magnetic mirror" effect on the neutrals, it is assumed in Figure 1 that the charge fraction is nearly 100% H, that is, the particle spends almost all its time as an H atom, and only occasionally loses its electron for a brief time. Each time it becomes a proton, its azimuthal velocity is redirected

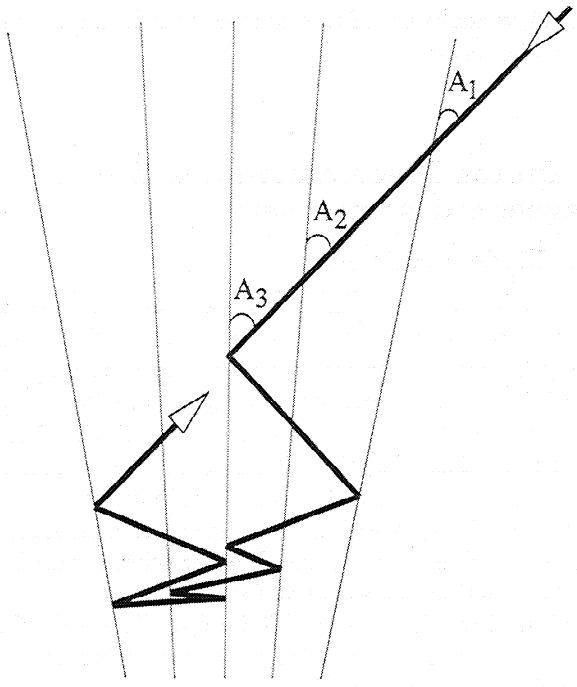

Figure 1. Illustration of "magnetic mirroring" for energetic atoms. Thin lines represent magnetic-field lines. The thick line represents trajectory of the particle. In this illustration the energetic particle is assumed to spend almost all its life in the form of a hydrogen atom, but it is randomly transformed for brief moments to a proton through temporary loss of an electron. During each such moment its velocity component perpendicular to the magnetic field is redirected (see text). Between successive redirections the angle between the particle trajectory and the magnetic field continually changes, that is, $A_1 < A_2 < A_3$.

in the plane perpendicular to the magnetic field. In our two-dimensional Figure 1 the redirection is an integral multiple of π radians, meaning that the particle either continues straight ahead after recapturing an electron, or else is reflected off the magnetic-field line. The pitch angle does not change upon reflection, but rather changes continually between reflections, as noted, for example, by the progression from angles A_1 to A_2 to A_3 in Figure 1. The particle eventually ends up with an upward velocity component, provided that it has not lost all its energy through collisions.

The equality of the mirror effect for both protons and hydrogen atoms leads to certain simplified concepts when analyzing proton precipitation into the atmosphere. To evaluate the pitch angle variations of a single energetic particle in the nonuniform magnetic field, it is not necessary to know whether the particle is charged or not at any particular time. Under the idealized conditions of the numerical model whose results are presented in section 3, that is, assuming nearly vertical magnetic field lines with horizontally uniform values of $(1/B)\times\partial B/\partial s$, and neglecting collisional changes in the pitch angle, the mirror altitude of any energetic particle depends only on its pitch angle at the top of the atmosphere, just as for a collisionless proton. In section 3.3 we make use of this concept to help understand the model results.

3. Proton Precipitation in a Dipolar Magnetized Atmosphere

3.1. Model and Inputs

To examine the quantitative influences of angular redistribution of hydrogen atoms in a nonuniform magnetic field, we use the transport code developed by *Galand* [1996], which solves the steady state Boltzmann equations for protons and H atoms. The particle fluxes are computed as a function of altitude, energy, and pitch angle (the latter defined to be zero for upgoing field-aligned particles), starting from a specified incident flux at the top of the atmosphere. The solution is based on the introduction of dissipative forces to describe the energy loss through collisions [*Galand et al.*, 1997]. This approach allows a simple way of introducing angular redistribution processes like the magnetic mirror into the transport equations. *Galand et al.* [1998] used this transport code to study the effect of magnetic mirroring on protons. Here we apply magnetic mirroring not only to protons but also to H atoms by introducing the relation (8) derived in section 2 into the H atom transport equation [*Galand et al.*, 1997, equation (8b)], using a term identical to the second term of equation (8a) of *Galand et al.* [1997]. A dipolar magnetic field is used to calculate the convergence of the magnetic field lines, but curvature is ignored, since in the high-latitude auroral regions the dip angle varies less than 0.8° from 100 to 800 km. For simplicity, calculations are carried out for a dip angle of 90°.

The incident flux at the top of the atmosphere is assumed to be purely protons, isotropic over the downward hemisphere, with a Maxwellian distribution in energy. The characteristic energy of the Maxwellian, E_0, is varied from 1 to 20 keV, typical for auroral proton precipitation [*Hardy et al.*, 1989]. The total incident energy flux integrated over pitch angle and energy, Q_0, is arbitrarily chosen as 1 erg cm^{-2} s^{-1}. The neutral atmosphere model is given by MSIS 90 [*Hedin*, 1991], for 70° latitude and 1900 local time in winter, with a magnetic activity index A_p of 20 and a solar $F_{10.7}$ index of 150, representative of average magnetic and solar conditions. The exospheric temperature is 1050 K. The collision cross-section set used is from *Basu et al.* [1987] and from *Rees* [1989]. The collisional energy losses are those presented by *Galand et al.* [1997]. The incident beam is assumed to be sufficiently broad that beam spreading associated with the horizontal diffusion of the hydrogen atoms can be neglected. No field-aligned electric field is considered. Because we wish to focus on the effects of magnetic mirroring in the present study, collisional angular redistribution is also neglected. The only source of angular redistribution is induced by the convergence of the magnetic-field lines acting on both protons and H atoms. As for numerical inputs, the altitude grid extends from 800 down to 100 km on 180 levels. The minimum energy of the energy grid is taken equal to 100 eV, and the maximum energy depends on the chosen E_0: The number of levels for the energy grid is between 100 and 200. The pitch angle cosine grid is uniform with 30 levels.

Before performing runs with collisions, we first checked that the magnetic mirroring of H atoms was introduced correctly in the code. Analogous to the test of *Galand et al.* [1998] on pure proton precipitation without collisions, we applied the code to pure H atom precipitation without collisions, with total reflection at the lower boundary. Under such conditions we can analytically determine the variation in altitude of μ for a particle, apply Liouville's theorem to get particle fluxes, and compare with the numerical transport solution. Because the magnetic term is independent of the charge value, we obtain exactly the same results as those presented by *Galand et al.* [1998], so we will not repeat them here. Note that in the absence of collisions and under the steady state assumption, an isotropic downward flux at the top of the atmosphere remains undiminished in strength at lower levels. If total absorption at the lower boundary were assumed, the upward flux would increase with increasing altitude, becoming isotropic over an increasing range of pitch angles less than 90°. Although the resulting net downward flux (downward - upward) per unit area would decrease with increasing altitude, the net particle flux through the height-varying cross section of a magnetic flux tube would be conserved.

3.2. Energy Conservation

For every run of the code, we check the energy conservation by evaluating whether the vertical energy flux divergence balances the energy lost at each level. The net energy flux into the top of a magnetic flux tube should equal the energy dissipated by collisions along the flux tube. Thus we modify the energy-conservation relation proposed by *Galand et al.* [1997], applicable in a uniform magnetic field, by including a factor proportional to the flux-tube cross section when integrating the energy loss and obtain

$$Q_0 - 2\pi \int_0^1 \mu \, d\mu \int E \, dE \sum_{X=\mathrm{H}^+,\mathrm{H}} \Phi_X(s_0, E, \mu) = 2\pi \int_0^{s_0} ds \sum_\alpha n_\alpha(s) \times \int_{-1}^1 d\mu \int dE \sum_{X=\mathrm{H}^+,\mathrm{H}} L_X^\alpha(E) \; \Phi_X(s, E, \mu) \left[\frac{B_0}{B(s)}\right], \quad (9)$$

where E is particle energy; Φ_X is the proton (X=H$^+$) or H atom (X=H) flux in cm^{-2} s^{-1} eV^{-1} sr^{-1}, obtained by solution of the Boltzmann equation; n_α is the neutral number density of the species α; L_X^α is the total energy loss function of the particle X colliding with the neutral species α, in eV cm^2; s_0 is the value of s at the upper boundary, equal here to the highest-altitude level, that is, to 800 km; and B_0 is the magnetic-field strength at that altitude. The cosine of the pitch angle, μ, is defined positive for upward particles. The first term on the left-hand side of (9) represents the downward energy flux incident at the top of the atmosphere, whereas the second term is the energy flux escaping from the atmosphere. The term on the right-hand side represents the total energy deposited through collisions in the atmosphere. For our simulations, the left- and right-hand sides of (9) balance numerically within 2%.

3.3. Albedo

To illustrate the influence of magnetic mirroring, we calculate the particle and energy albedos, defined as the fractions of incoming particles or incident energy flux that escape back out of the atmosphere. The particle albedo in percent is defined as

$$\alpha_P = 100 \times \frac{\int_0^1 \mu \, d\mu \int dE \sum_{X=\mathrm{H}^+,\mathrm{H}} \Phi_X(s_0, E, \mu)}{\int_{-1}^0 |\mu| \, d\mu \int dE \, \Phi_{\mathrm{H}^+}(s_0, E, \mu)}, \quad (10)$$

and the energy albedo in percent is defined as

$$\alpha_E = 100 \times \frac{2\pi \int_0^1 \mu \, d\mu \int E \, dE \sum_{X=\mathrm{H}^+,\mathrm{H}} \Phi_X(s_0, E, \mu)}{Q_0}. \quad (11)$$

In (10) the integration over the downward hemisphere (denominator) is applied only to protons, as the incident flux is assumed to be purely protons. In addition to evaluating the total albedos given by (10) and (11), we also evaluate their separate proton and H atom components, obtained by deleting the X = H or X = H$^+$

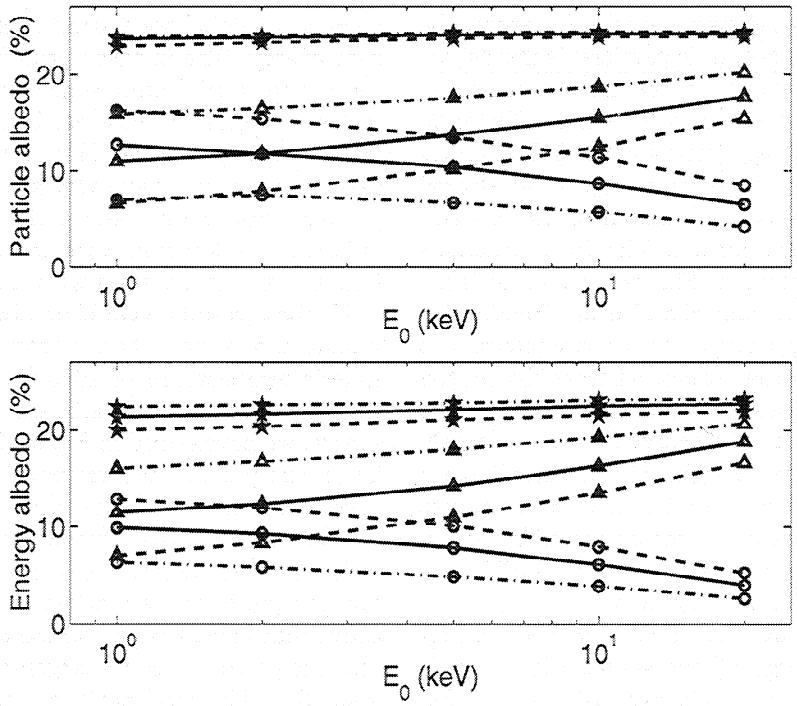

Figure 2. (a) Particle albedo (stars), proton albedo (triangles), and H atom albedo (circles) as a function of the characteristic energy E_0 of the incident flux, and for an atmosphere with an exospheric temperature of 1050 K (solid lines), of 700 K (dashed-dotted lines), and of 1300 K (dashed lines). (b) The same as Figure 2a except for energy albedo.

components, respectively, from the summations in the numerators. We verified that the results do not significantly depend on the dip angle for a range of reasonable high-latitude values; our calculations are for a dip angle of 90°.

The particle albedo is shown by the solid line with stars in Figure 2a. The particle albedo is relatively independent of the characteristic energy E_0 of the incident flux, varying by only 2.5% over the 1-20 keV range. To understand why, note the following considerations. It was pointed out in section 2 that each incident energetic particle has a well-defined mirroring height determined by its initial pitch angle, under the assumptions used in our calculations. For a given incident particle energy, if the initial pitch angle is close to 90°, the particles are reflected and escape the atmosphere, contributing to the albedo. For an initial pitch angle close to 180° the particles are absorbed in the atmosphere, losing all their energy through collisions. Numerically, particles whose energy falls below the minimum value of the energy grid, 100 eV, are considered permanently lost into the atmosphere. Increasing the pitch angle starting from 90°, we reach a critical pitch angle for which the particles are reflected but lose all their energy by the time they reach the top of the atmosphere. This critical pitch angle for which the particles do not escape the atmosphere is associated with a mirroring altitude, which we call the critical mirroring height. The critical mirroring height is lower for more energetic particles than for less energetic particles, but over the 1-20 keV range the difference is small in comparison with the distance to the upper boundary at 800 km, and so the change of critical incident pitch angle with energy is small. Consequently, the fraction of reflected energetic particles is insensitive to the incident energy, if one ignores their charge state. On the other hand, the other solid lines in Figure 2a show that the proton albedo (triangles) and the H atom albedo (circles) are very sensitive to E_0. After several charge-changing collisions the fractions of protons and H atoms approach an equilibrium. The charge fractions at the equilibrium, plotted in Figure 3 for an altitude of 300 km, show clearly that the H atom fraction increases with decreasing energy. As a consequence, the H atom albedo follows that trend, whereas the proton albedo varies in an opposite way as a function of E_0. Nevertheless, even though the charge fraction is largely in favor of H atoms at low energies, the proton albedo is dominant or at least close to that of H atoms, because a good fraction of the incident protons are mirrored before reaching those altitudes where charge equilibrium is attained, around 300 km and below.

The energy albedos are plotted as solid lines in Figure 2b. The total energy albedo shown with stars is relatively independent of the characteristic energy E_0, as is the total particle albedo. The small increase with increasing energy can be attributed to the variation of energy loss function with respect to energy and to the lower value of the critical mirror altitude for higher energies. The latter point implies that a larger fraction of incident pitch angles is reflected, as well as a smaller fraction of the incident energy lost for a given pitch angle. Indeed, whereas a 1 keV particle at the critical incident pitch angle loses 100% of its original energy, a 10 keV particle at that pitch angle loses much less than 100% of its incident energy. For a given E_0 the energy albedo is only modestly smaller than the particle albedo shown in Figure 2a since only the relatively small fraction of particles that penetrate almost to the critical mirroring height lose a significant portion of their incident energy. The incident proton beam tends to reach the charge equilibrium which favors H atoms mainly at low energies, as illustrated in Figure 3. Therefore, not only are there fewer H atoms present for high incident energies, but they carry much less energy than the protons. For these reasons, the proton energy albedo (triangles) is dominant over the H atom energy albedo (circles), and it increases with increasing energy.

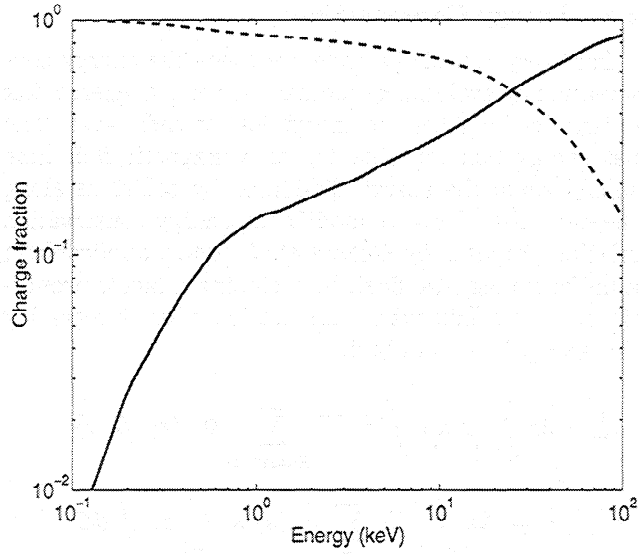

Figure 3. Proton fraction (solid line) and H atom fraction (dashed line) for charge equilibrium at an altitude of 300 km, as a function of the particle energy.

All these results have been obtained with the atmospheric model described in section 3.1, with an exospheric temperature of 1050 K. In order to estimate the dependence of the albedos on the neutral atmosphere, we have added in Figure 2 the albedos obtained for an exospheric temperature of 700 K (dashed-dotted lines) and those for an exospheric temperature of 1300 K (dashed lines). If the atmosphere is cooler, it contracts such that the neutral densities decrease. Therefore, charge equilibrium is reached at a lower altitude, and, above that level, the proton fraction is higher. As a result, the proton albedo is larger, and the H atom albedo is smaller. The total particle albedo is not sensitive to the atmospheric temperature since the changes in critical mirroring height are insufficient to produce any significant change in the critical incident pitch angles for reflected particles. For a higher exospheric temperature

the atmosphere expands, and thus the opposite behavior for the albedos is observed.

Returning to the initial atmosphere with an exospheric temperature of 1050 K, we also computed the albedos using the term proposed by *Kozelov* [1993] for the magnetic mirroring of H atoms when the field lines are radial, which effectively corresponds to a magnetic monopole configuration. The deduced particle and energy albedos are plotted with dashed lines in Figure 4a and 4b, respectively. The albedos obtained previously with the term derived from (8) have been added in solid lines. The term used by *Kozelov* [1993] for monopolar magnetic field lines is 2/3 that obtained with an H pitch angle referenced to dipolar magnetic field lines. Therefore, with the Kozelov term, the H atom albedo is smaller, and since the H fraction becomes more and more significant with decreasing energy, the total albedo is reduced to a greater extent when the incident energy is small. As a result, the particle albedo is relatively more sensitive to E_0 with the Kozelov term. As for the energy albedo, the same conclusion can be drawn. Finally, it should be noted that *Kozelov* [1993] found values much smaller than those obtained in the present study for the total particle and energy albedos. This can be attributed mainly to a different atmospheric model (only N_2 for Kozelov) and to a lower upper boundary (only 700 km for Kozelov), and, to a lesser extent, to a different cross-section set and a different incident flux (monoenergetic for Kozelov).

4. Discussion and Conclusions

Our primary purpose has been to point out that the "magnetic mirror" effect can under certain circumstances be applied equally to energetic neutral and charged particles, and to give a new perspective on the nature of the magnetic mirror effect. That effect can be viewed as arising purely from the movement of a particle through a nonuniform magnetic field, irrespective of the particle's charge. From this perspective, the function of the magnetic field is only to confine a charged particle to the vicinity of a particular field line while its pitch angle is changing.

A relevant step in studying numerically the effect of a magnetic field on both protons and H atoms is to check the energy conservation. We point out that in the presence of a nonuniform magnetic field, one needs to take into consideration the variation of the magnetic flux tube cross section in the terms accounting for the energy deposition through collisions in the atmosphere.

Since observations from space of upward H atom fluxes are possibly relevant to inferring information about the proton aurora, we have estimated not only the total particle and energy albedos but also those for each charge state. The total particle albedo is nearly independent of the incident energy of the particles. However, because the charge fraction at equilibrium favors neutral particles at low energies but protons at high energies, the H atom albedo decreases, whereas the proton albedo gets larger with increasing energy. As for the

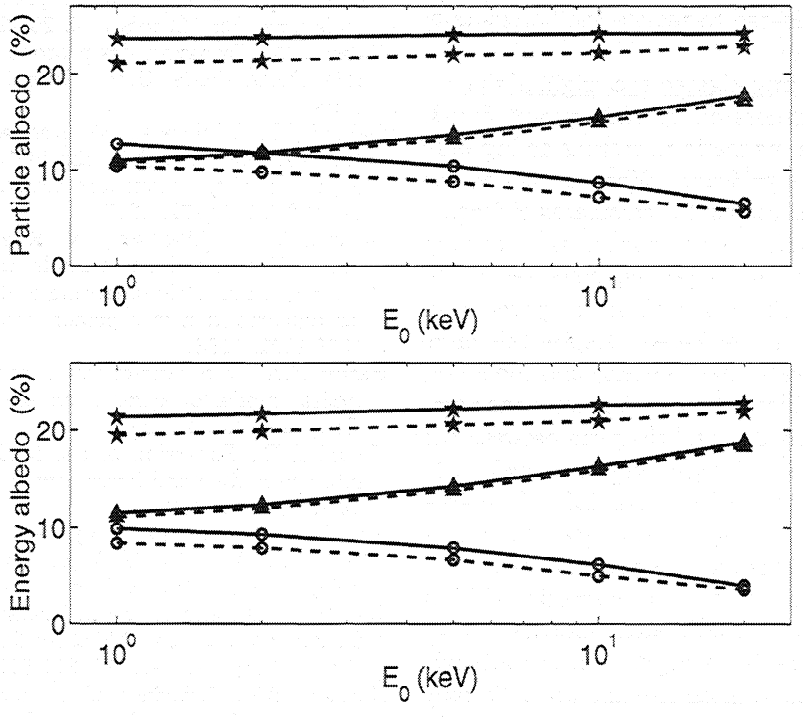

Figure 4. (a) Particle albedo (stars), proton albedo (triangles), and H atom albedo (circles) as a function of the characteristic energy E_0 of the incident flux, for an atmosphere with an exospheric temperature of 1050 K. The solid lines are the results using the dipolar magnetic configuration for H atom mirroring and the dashed lines are the results using the monopolar configuration used by *Kozelov* [1993]. (b) The same as Figure 4a except for energy albedo.

energy albedo, because the percentage energy lost by a particle of given incident pitch angle decreases as the incident energy increases, the energy albedo increases with increasing energy, though only weakly so. Because H atoms are preferentially produced mainly at low energies, the H atom albedo is reduced, whereas the proton energy albedo increases significantly with increasing energy. We show also that the atmospheric model does not have a large influence on the total particle and energy albedos but does influence the albedos associated with each charge state.

Quantitatively, our new relation for pitch angle changes of H atoms produces modest increases in the calculated particle and energy albedos of an incident proton flux in a dipolar magnetic field, compared with the relation of *Kozelov* [1993], who effectively used a monopolar field for the H atoms. The difference between the calculated total albedos increases with decreasing energy of the incident particles since the fraction of H atoms at charge equilibrium increases with decreasing energy.

We note that magnetic mirroring does not affect seriously the electron production rate in the energy deposition region, that is, in the 100-200 km altitude range. The fact that part of the incident energy flux is lost to albedo does not significantly affect the energy fluxes at lower levels in the model because the convergence of magnetic-field lines channels the remaining downgoing particles into a more concentrated area, offsetting the loss. Only when the finite horizontal extent of a realistic particle flux is taken into consideration can the energy loss to albedo be considered to reduce the horizontally averaged ionization rate.

Galand et al. [1998] investigated the origin of the red shift of H emissions generated by the upward fluxes. They showed that the magnetic mirroring acting only on protons cannot be significant. When we added the magnetic mirroring of H atoms, the calculated Hβ intensity at zero Doppler shift, that is, the emission coming from H atoms at their mirror points, increased up to almost 400% for E_0 equal to 1 keV, as compared with proton-only mirroring. Nevertheless, despite this large increase, the ratio between that intensity and the intensity at the line peak (which is blue shifted from the nominal line position) is only 3%, and the ratio between the total red-shifted emission, integrated over wavelength, to the total Hβ emission is less than 1%. Therefore the role played by the magnetic field in generating red-shifted hydrogen emissions remains very modest.

The present study shows that the magnetic field has a major effect on proton and H atom albedos. However, the values obtained here depend on the altitude chosen for the top of the atmosphere and are valid only for an incident flux assumed to be isotropic over the downward hemisphere. In addition, we have not considered collisional angular redistribution; even though acting mainly at low altitudes, it contributes to the generation of an upward flux. Moreover, the spreading as well as a possible field-aligned electric field have been neglected. Finally, we assume the azimuthal isotropy around the magnetic-field lines, so our one-dimensional-in-space model is incapable of simulating the azimuthal anisotropy of the particle flux observed by *Søraas and Aarsnes* [1996]. Our model results should be treated more as illustrations of physical processes than as accurate quantitative predictions of realistic albedos.

Acknowledgments. We thank Tom Bogdan and a referee for insightful comments on earlier drafts. M.G. gratefully acknowledges the financial support of the Advanced Study Program and the High Altitude Observatory, divisions of the National Center for Atmospheric Research (NCAR). NCAR is sponsored by the National Science Foundation.

Janet G. Luhmann thanks Charles S. Deehr and Harlan E. Spence for their assistance in evaluating this paper.

References

Basu, B., J.R. Jasperse, R.M. Robinson, R.R. Vondrak, and D.S. Evans, Linear transport theory of auroral proton precipitation: A comparison with observations, *J. Geophys. Res.*, *92*, 5920-5932, 1987.

Basu, B., J.R. Jasperse, D.J. Strickland, and R.E. Daniell, Transport-theoretic model for the electron-proton-hydrogen atom aurora, 1, Theory, *J. Geophys. Res.*, *98*, 21,517-21,532, 1993.

Chen, F.F., *Introduction to Plasma Physics and Controlled Fusion*, vol. 1, 2nd ed., Plenum, New York, 1983.

Deehr, C.S., D.A. Lorentzen, F. Sigernes, and R.W. Smith, Dayside auroral hydrogen emission as an aeronomic signature of magnetospheric boundary layer processes, *Geophys. Res. Lett.*, *25*, 2111-2114, 1998.

Eather, R.H., Auroral proton precipitation and hydrogen emissions, *Rev. Geophys.*, *5*, 207-285, 1967.

Galand, M., Transport des protons dans l'ionosphere aurorale, Ph.D. thesis, Univ. Grenoble I, Grenoble, France, 1996.

Galand, M., J. Lilensten, W. Kofman, and R.B. Sidje, Proton transport model in the ionosphere, 1, Multistream approach of the transport equations, *J. Geophys. Res.*, *102*, 22,261-22,272, 1997.

Galand, M., J. Lilensten, W. Kofman, and D. Lummerzheim, Proton transport model in the ionosphere, 2, Influence of magnetic mirroring and collisions on the angular redistribution in a proton beam, *Ann. Geophys.*, *16*, 1308-1321, 1998.

Hardy, D.A., M.S. Gussenhoven, and D. Brautigam, A statistical model of auroral ion precipitation, *J. Geophys. Res.*, *94*, 370-392, 1989.

Hedin, A.E., Extension of the MSIS thermosphere model into the middle and lower atmosphere, *J. Geophys. Res.*, *96*, 1159-1172, 1991.

Henriksen, K., N.I. Fedorova, G.F. Totunova, C.S. Deehr, G.J. Romick, and G.G. Sivjee, Hydrogen emissions in the polar cleft, *J. Atmos. Terr. Phys.*, *47*, 1051-1056, 1985.

Jasperse, J.R., and B. Basu, Transport theoretic solutions for auroral proton and H atom fluxes and related quantities, *J. Geophys. Res.*, *87*, 811-822, 1982.

Kozelov, B.V., Influence of the dipolar magnetic field on transport of proton-H atom fluxes in the atmosphere, *Ann. Geophys.*, *11*, 697-704, 1993.

Lie-Svendsen, Ø., and M.H. Rees, An improved kinetic model for the polar outflow of a minor ion, *J. Geophys. Res.*, *101*, 2415-2433, 1996.

Lilensten, J., and M. Galand, Proton-electron precipitation

effects on the electron production and density above EISCAT (Tromsø) and ESR, *Ann. Geophys.*, *16*, 1299-1307, 1998.

Lorentzen, D.A., F. Sigernes, and C.S. Deehr, Modeling and observations of dayside auroral hydrogen emission Doppler profiles, *J. Geophys. Res.*, *103*, 17,479-17,488, 1998.

Mihalas, D., and B.W. Mihalas, *Foundations of Radiation Hydrodynamics*, Oxford Univ. Press, New York, 1984.

Rees, M.H., *Physics and Chemistry of the Upper Atmosphere, Cambridge Atmos. Space Sci. Ser.*, Cambridge Univ. Press, New York, 1989.

Senior, C., J.R. Sharber, O. de la Beaujardière, R.A. Heelis, D.S. Evans, J.D. Winningham, M. Sugiura, and W.R. Hoegy, *E* and *F* region study of the evening sector auroral oval: A Chatanika/Dynamics Explorer 2/NOAA 6 comparison, *J. Geophys. Res.*, *92*, 2477-2494, 1987.

Sigernes, F., G. Fasel, J. Minow, C.S. Deehr, R.W. Smith, D.A. Lorentzen, L.T. Wetjen, and K. Henriksen, Calculations and ground-based observations of pulsed proton events in the dayside aurora, *J. Atmos. Terr. Phys.*, *58*, 1281-1291, 1996.

Søraas, F., and K. Aarsnes, Observations of ENA in and near a proton arc, *Geophys. Res. Lett.*, *23*, 2959-2962, 1996.

Søraas, F., H.R. Lindalen, K. Måseide, A. Egeland, T.A. Sten, and D.S. Evans, Proton precipitation and the H_β emission in a postbreakup auroral glow, *J. Geophys. Res.*, *79*, 1851-1859, 1974.

M. Galand, National Oceanic and Atmospheric Administration, Space Environment Center, 325 Broadway, Boulder, CO 80303. (galand@sec.noaa.gov)

A. D. Richmond, High Altitude Observatory, National Center for Atmospheric Research, 3450 Mitchell Lane, Boulder, CO 80307-3000.

(Received September 14, 1998; revised November 3, 1998; accepted November 13, 1998.)